Carbon Nanotubes Networking in Styrene-Butadiene Rubber: A Dynamic Mechanical and Dielectric Spectroscopy Study

Daniela García, Martina Salzano de Luna, Giuseppe Mensitieri, Mariano Escobar, Marcela Mansilla,* and Antonio Baldanza*

The study of the reinforcement network in elastomer compounds is one of the most relevant issues for the application of these materials because their properties are strongly dependent on the obtained morphology. To this regard, the viscoelastic and dielectric behavior of vulcanized styrene butadiene rubber (SBR) reinforced with different amounts of carbon nanotubes (CNT) have been investigated and compared with the vulcanized unfilled SBR and the vulcanized SBR samples reinforced with a conventional amount of carbon black (40 phr). Differential scanning calorimetry (DSC) measurements have been carried out to highlight possible differences of the glass transition temperatures for all the reinforced compounds. The percolation threshold value of the nanocomposite samples has been estimated by dielectric analysis. Finally, dynamic mechanical analysis (DMA) measurements have been performed in tensile mode in the temperature range of −60 to 80 °C to obtain both E' and E''. From these experimental data, the master curve for each sample has been estimated by using the time–temperature superposition principle in combination with the vertical shift approach. From the analysis of this latter, the activation energy, associated to the thermal movement of the reinforcement network, has been calculated to better elucidate the reinforcement mechanism in the nanocomposites.

1. Introduction

Styrene-butadiene rubber (SBR) is one of the most important polymers used in the tire industry. It presents high filler-loading capacity, which is fundamental to obtain good mechanical and dynamical properties. Carbon black (CB) and precipitated silica are the conventional fillers used in rubber compounds. In the last years, a considerable number of works have been devoted to study the incorporation of alternative nano reinforcements in elastomer compounds. Carbon nanotubes (CNT) are one of the more suitable candidates to replace, totally or partially, carbon black (CB), thus allowing the reduction of the filler content without diminishing the mechanical performance.[1–8]

The improvements achieved in the final properties of the reinforced materials are strongly influenced by the particle–polymer interaction degree, which in turn depends on several factors, such as size and geometry of the particle, degree of dispersion and energetic distribution of the surface.[9,10] In the case of elastomers reinforced with CB, there is an intensive polymer–filler interaction, and polymer chains anchor to the filler surface. Therefore, elastomer chains form a shell around the reinforcement with a filler-like stiffness and a glassy-like behavior, which, consequently, lead to an increase of the volume of the filler.[10] The presence of a polymer layer with glassy-like behavior next to filler surface and an outer phase displaying a gradient of mobility has been confirmed by different techniques, such as NMR[11,12] and mechanical analyses.[13,14]

D. García
Department of Technical Assistance to the Rubber Industry
National Institute of Industrial Technology (INTI)
Av. General Paz 5445, San Martin B1650WAB, Argentina

M. Salzano de Luna, G. Mensitieri, A. Baldanza
Department of Chemical
Materials and Production Engineering
University of Naples Federico II
Piazzale Tecchio 80, Naples 80125, Italy
E-mail: antonio.baladanza@unina.it

M. Escobar
Technical Department of Advanced Materials
National Institute of Industrial Technology (INTI) | CONICET
Av. General Paz 5445, San Martin B1650WAB, Argentina

M. Mansilla
Technical Department of Advanced Materials
National Institute of Industrial Technology (INTI)
Av. General Paz 5445, San Martin B1650WAB, Argentina
E-mail: mmansilla@inti.gob.ar

The ORCID identification number(s) for the author(s) of this article can be found under https://doi.org/10.1002/mame.202200514

A powerful tool to study the structure of the filler network in an elastomeric compound is the dielectric relaxation spectroscopy (DRS).[15–19] Regarding simple systems, Liu et al. analyzed the structure of deproteinized natural rubber (NR) by this technique, finding a new relaxation mode which is four orders of magnitude slower than the normal mode and it is associated to the relaxation of free mono- or diphosphate groups.[20] Wu et. al. studied more complex systems: graphene oxide (GO) and butadiene-styrene-vinyl pyridine rubber (VPR) compounds were prepared by a co-coagulation process.[21] They used different flocculants: hydrogen chloride and calcium chloride (HVPR and CaVPR, respectively), to form two kinds of bonding interfaces (an ionic and a hydrogen bonding). Through DRS, it can be identified two distinct relaxation processes, segmental relaxation and interfacial relaxation. It was found that the GO concentration does not affect the segmental dynamics of CaVPR, but the segmental dynamics of the HVPR slows down at 1.5 vol% of GO. Meanwhile, the segmental relaxation of HVPR is always a little faster than its CaVPR counterpart. Subramanian et al. analyzed polychloroprene rubber reinforced with CNT treated with an ionic liquid by dielectric measurements, showing that the filler dispersion and the conductivity of the compound are improved when modified CNTs are used.[22] In fact, both the surface state of the CNTs and the method of incorporation into the rubber matrix are factors that determine the final properties of the compound. For example, Peddini et al. characterized the behavior of SBR and oxidized CNT compounds in detail using various experimental techniques.[23] The surface modification of the CNT alters its surface energy, which increases its reactivity and facilitates its union with the rubber matrix. On the other hand, before the incorporation in the SBR matrix, oxidated CNTs need to be dispersed in a solvent, which makes the process less feasible for the tire manufacturing industry.

Regarding the dynamic properties of rubber compounds, they are of great interest since some tire properties, such as wet grip and rolling resistance, are closely related to loss tangent values. However, there is a major drawback: the frequency range available for measurements is quite narrow due to the instrumental limitation, which prevents the investigation of molecular dynamics in detail. It is well known that the concept of time-temperature superposition (TTS) allows to characterize the behavior of the rubber under an extended frequency range, which, otherwise, would be hardly accessible by performing a single isothermal test.[24] Generally, the TTS is applied to a series of isothermal curves of the complex modulus G^* (or, equivalently, E^*) estimated with frequency sweep tests at different temperatures. Within this temperature interval, a reference temperature (T_0) is chosen to characterize the response of the material. According to TTS, the master curve is obtained by applying horizontal shifts on each curve to extend the frequency range of the measured curve at T_0 (that remains fixed). Xiang et al.[25] performed the TTS procedure to obtain master curves on unfilled SBR compounds aged at 130 °C with aging periods of 1, 2, and 4 d. This treatment allowed them to demonstrate the effect of enhanced intermolecular coupling and severe cross-linking during aging, due to thermal decomposition of polysulfidic crosslinks to form more mono and disulfidic ones, leading to an increase of the crosslinks density. In the case of reinforced samples, it was found that a horizontal shift along the time or frequency axis is not enough to obtain a smooth curve. In particular, the difficulties of overlapping between the curves are more frequent in the low frequency range, where the response of the compound is governed by the reinforcement network, a fraction of which is submitted to irreversible break-down when successive strain cycles are applied.[10]

In the present contribution, with the aim of transferring the SBR/CNT nanocomposites into the tire industry, a thorough dynamic-mechanical analysis has been performed on SBR/CNT nanocomposites (with different amounts of CNTs) obtained by mixing processes similar to the ones already used in tire industries. For the sake of comparison, unfilled SBR and SBR filled with CB (40 phr) have been also investigated. The percolation threshold for CNT filled samples has been estimated by means of dielectric spectroscopy. Moreover, differential scanning calorimetry (DSC) measurements were carried out to study the vulcanization reaction and determine the glass transition temperature (T_g). Finally, master curves were generated for all the compounds at 0 °C, which is a temperature with technical relevance in the tire industry due to its relationship with wet grip efficiency.[26–28] The vertical shift factor applied to each isothermal curve allowed to estimate the activation energy associated with the mobility of those chains attached on the filler surface (bound rubber).

2. Experimental Section

2.1. Materials

The rubber matrix is SBR-1502 (kindly provided by Pampa Energía, Argentina) and was compounded using a two–roll mill with the following curing reagents: 2 phr of sulfur as vulcanizing agent, 2 phr of CBS (N-cyclohexyl-2-benzothiazolesulfenamide), and 0.5 phr of TMTD (tetramethyl thiuram disulfide) as primary and secondary accelerators respectively, 2 phr of stearic acid and 3 phr of zinc oxide as activators; 1.5 phr of aromatic oil was also added as a processing aid. All these ingredients are technical grade due to its industrial application. As reinforcement particles, multiwall carbon nanotubes (Nanocyl 7000, 90 % carbon purity) and CB N330 were used.
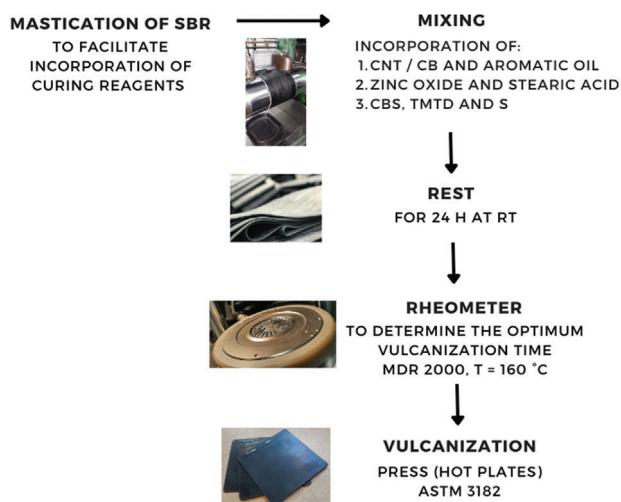
2.1.1. Sample Preparation

The preparation technique of the samples was the following: first the SBR was masticated and then the reinforcement particles were incorporated. Then vulcanization agents were added in this order: aromatic oil, stearic acid, zinc oxide, CBS, TMTD, and sulfur (S). Once the incorporation of the additive was finished, the compound was calendered to increase the homogeneity. Finally, the compound was left at room temperature (RT) for 24 h prior to the vulcanization characterization. **Figure 1** shows a diagram of the different steps to obtain the vulcanized compounds.

2.1.2. Sample Vulcanization

The vulcanization reaction was performed in a rheometer MDR-2000 (Alpha Technologies) at 160 °C, and the optimum vulcanization time was obtained (at which the maximum torque is

COMPOUND PREPARATION

MASTICATION OF SBR
TO FACILITATE INCORPORATION OF CURING REAGENTS

MIXING
INCORPORATION OF:
1. CNT / CB AND AROMATIC OIL
2. ZINC OXIDE AND STEARIC ACID
3. CBS, TMTD AND S

REST
FOR 24 H AT RT

RHEOMETER
TO DETERMINE THE OPTIMUM VULCANIZATION TIME
MDR 2000, T = 160 °C

VULCANIZATION
PRESS (HOT PLATES)
ASTM 3182

Figure 1. Diagram showing the typical steps involved to obtain vulcanized rubber sheets according to ASTM D3182.

reached). Then, the compounds were press-cured at 160 °C up to the determined time to obtain 2 mm thick sheets according to ASTM D3182 – 16 (last step on Figure 1). On those vulcanized samples the different characterization techniques were performed.

2.2. Experimental Methods

2.2.1. DSC

The measurements were performed using a DSC Q-20 (TA instruments, Waters Co., New Castle, DE, USA) with a heating rate of 5 °C min^{-1}. First, the vulcanization reaction on uncured samples was characterized by a temperature sweep test from 25 to 200 °C. Then, on vulcanized samples, the glass transition temperature was estimated with a temperature sweep test from −70 up to 0 °C, with the same heating rate. In all measurements, the weight of the sample was in the range 10–15 mg.

2.2.2. Dynamic Mechanical Analysis (DMA)

DMA measurements were performed on vulcanized samples, in tensile mode with 1% of elongation strain to evaluate the complex modulus E* using a DMA+1000 Metravib (by ACOEM, Limonest, France SAS). To obtain the master curves of the compounds at $T_0 = 0$ °C, isothermal frequency sweep tests between 0.8 and 30 Hz were performed at temperatures between −35 and 30 °C.

In addition, DMTA measurements at 10 Hz were performed on Rheometric SCI, from −60 to 30 °C, with a heating rate of 2 °C min^{-1} to analyze the temperature dependence of the storage modulus (E′) and tan δ. A static prestrain of 1% was applied and the dynamic load amplitude was 0.1% of strain.

2.2.3. Dielectric Relaxation Spectroscopy

Dielectric relaxation spectroscopy was performed using a rotational rheometer (ARES, Rheometrics Scientific), constituted by a couple of parallel stainless-steel plates (diameter 25 mm) connected to an LCR Meter (E4980A, Agilent). Measurements were performed on 2 mm thick sheets. For each sample, three independent measurements were carried out. A constant compressive force was applied to the samples during the tests to ensure contact between the sheet and the parallel plates. The dielectric response was measured at room temperature and the real (ϵ') and imaginary (ϵ'') parts of the complex permittivity were obtained as a function of the frequency (ω) of the applied alternating electrical field, in the range $10^1 - 10^4$ Hz. The dielectric constant, ϵ_c, and the real part of the complex conductivity, σ', were also calculated by Equations (1) and (2), respectively

$$\epsilon_c = \frac{\epsilon'}{\epsilon_0} \tag{1}$$

$$2\sigma' = \epsilon_0 \epsilon'' \omega \tag{2}$$

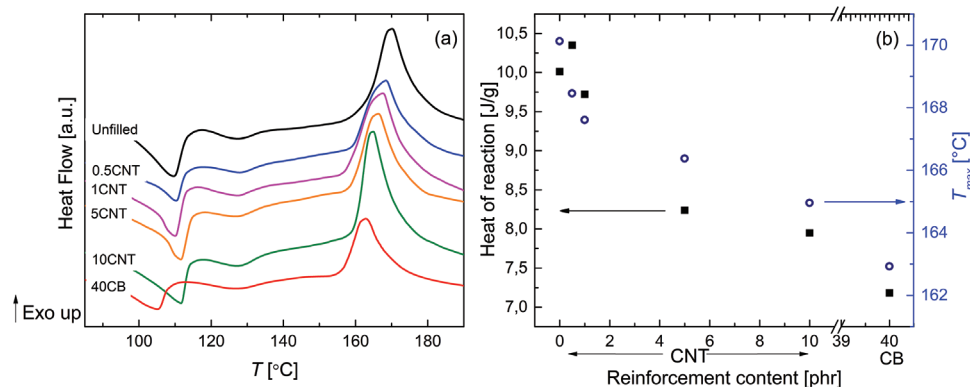Being $\epsilon_0 = 8.85 \times 10^{-12}$ F m^{-1} the permittivity of free space.

From the analysis of σ' as a function of ω, the DC conductivity was estimated at low frequencies, where a plateau is reached. This extrapolated value, σ_0, increases as a function of the filler content and allows the estimation of a percolation threshold value.

3. Results and Discussion

3.1. Differential Scanning Calorimetry

Figure 2a shows the thermograms obtained to characterize the vulcanization reaction of the samples by DSC. In these unvulcanized compounds, the molecular movement depends on the interaction between the reinforcement particles and rubber chains and on the inter- and intramolecular interactions, being all of them influenced by the temperature. In the thermograms, all the samples present an endothermic peak in the range 105–111 °C, which can be attributed to the formation of the highly active zinc stearate salt from the reaction of ZnO with stearic acid and the release of water as a sub-product [29] and, also, to the melting point of sulfur.[30] This peak occurs at lower temperature in the case of 40CB. On the other hand, the vulcanization reaction is manifested by the exothermic peak. The temperature values at which this exothermic peak occurs for the different samples are in the range 160–170 °C and can be observed that the reaction takes place at lower temperature when the amount of reinforcement increases. This can be attributed to an enhancement of the thermal conductivity in the compound with the CNT content and with the incorporation of CB, due to the higher thermal conductivity of these particles in comparison with the SBR matrix (which is a thermally insulating material).[31–33]

The values of the vulcanization heat and of the temperature corresponding to the maximum of the exothermic peak were determined from Figure 2a and are shown in Figure 2b. The value of the vulcanization heat per gram decreases with the filler loading,

ADVANCED
SCIENCE NEWS
www.advancedsciencenews.com

[M] acro-
molecular
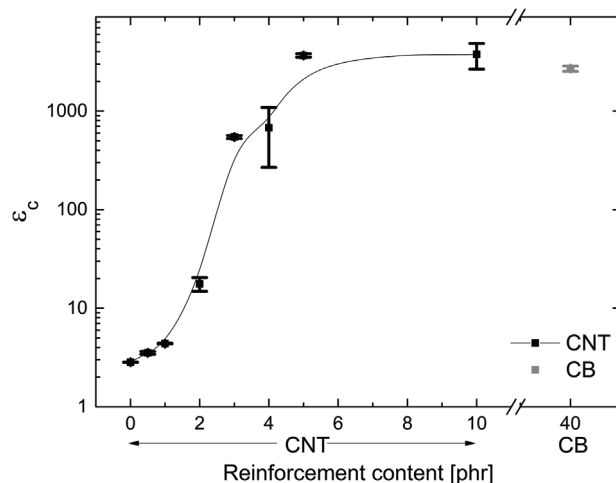Materials and Engineering
www.mame-journal.de

Figure 2. a) Heat flow as function of temperature measured by DCS on uncured samples to characterize the vulcanization reaction, b) Heat of reaction and maximum temperature at the vulcanization peak, determined from (a) around 160–170 °C.

Table 1. Glass transition temperature values determined by DSC for the vulcanized SBR compounds. The obtained values are not significantly different.

Compound	T_g [°C]
Unfilled	−50.2 ± 2.1
0.5CNT	−50.0 ± 1.3
01CNT	−51.2 ± 1.9
5CNT	−51.8 ± 1.2
10CNT	−51.9 ± 1.4
40CB	−53.3 ± 2.7

Figure 3. Dielectric constant at low frequency as a function of the filler content. Lines are to guide the eye. Black and gray squares correspond to samples containing CNT and CB, respectively.

indicating fewer chemical reactions as the reinforcement content increases. This could be explained by the fact that the CNT particles immobilize part of the rubber chains to be crosslinked and also absorb a fraction of the curing reagents, generating a lower conversion of the reaction.[34] In a previous work, the activation energy of the reaction (E_{act}^R) was determined for some of these compounds through rheometric measurements performed at different temperatures and applying a kinetic model to obtain the vulcanization rate.[1] It was found that the E_{act}^R increases with the filler amount, so more energy is needed to overcome the mobility restrictions to proceed with the crosslinking reactions. Furthermore, the percentage of the vulcanizing reagents decreases gradually in the compound when the amount of CNT increases, therefore the heat released decreases. The same behavior was found by Hosseini et al. in SBR/silica samples,[35] Zhou et al. in SBR/CNT nanocomposites[36] and by Wu et al. in natural rubber/graphite oxide samples.[30] In addition, Wu et al. studied the kinetic of the reaction by DSC in a system made of vulcanizing agents with different amounts of reinforcing particles in the absence of rubber. They obtained that the incorporation of filler decreases the exothermic peak (that corresponds to the crosslinking reaction) from 164 to 124 °C.

The glass transition temperature (T_g) has been estimated in vulcanized samples by locating the change in enthalpy. For the sake of brevity, the plot of the thermograms is omitted and only the obtained values are reported in **Table 1**, showing that the transition from the glassy 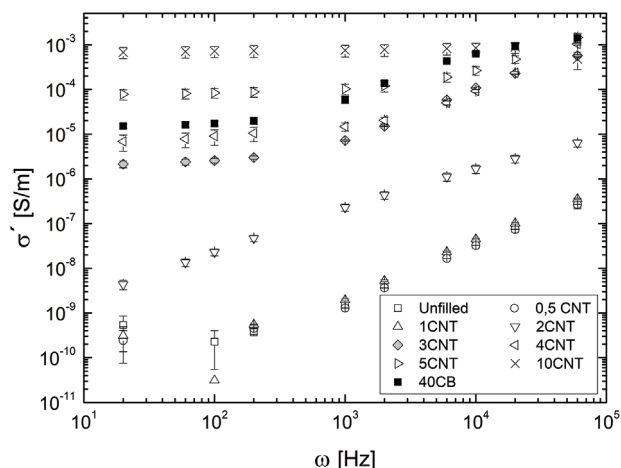to the rubbery state occurs at a similar temperature in all the compounds, regardless of the type and the amount of reinforcement.

3.2. Dielectric Properties

It is known that CNTs are electrical conductors, and the SBR is an insulating material. However, if the filler content is high enough, a 3D network of CNT could be formed that extends throughout the rubber matrix, which would significantly affect the electrical behavior of the whole sample.[2,37] In particular, the presence of conductive CNT radically affects the dielectric response of the rubber matrix.[38–40]

The dielectric constant, ϵ_c, measured at the lowest frequency investigated (i.e., 20 Hz) is reported in **Figure 3** as a function of filler content. An increase of ϵ_c with the amount of filler is appreciated, and the observed trend suggests a transition from one regime to another at around 2 phr of CNT. This pronounced enhancement in effective permittivity of the nanocomposites near the percolation threshold can be explained according to the interfacial polarization (Maxwell–Wagner–Sillar effect) due to the

**ADVANCED
SCIENCE NEWS**

www.advancedsciencenews.com

{M acro-
olecular
Materials and Engineering

www.mame-journal.de

Figure 4. Real part of the complex conductivity as a function of frequency for each compound.

presence of microcapacitor cosituted by clusters of nanoparticles isolated by very thin layers of polymer. The latter increase the intensity of the local electric filed just around the conductive fillers, eventually promoting the accumulation of charge carriers at the fillers–matrix interface.[41,42]

More accurate information on the formation of a conductive space-spanning network of particles can be gathered by looking at the frequency dependence of the real part of the complex conductivity, s', in **Figure 4**.

When the filler content is high enough, s' flattens out at low frequencies, reaching a plateau value s_0. It gives an estimate of the electrical conductivity which would be measured under direct conditions and thus suggests the formation of the CNT network throughout the rubber matrix. For each compound, the values of s_0 were estimated by successfully fitting the universal AC law equation[43] to the experimental data of s' in Figure 4

$$\sigma' = \sigma_0 + A \times w^s \qquad (3)$$

being A the scaling constant and s the critical exponent. When the filler content is above the percolation threshold, ϕ_c, a conductive network is created throughout the volume of the insulating matrix, bringing a sudden increase in the electrical conductivity. This transition can be appreciated by looking at the values of s_0 and s as a function of filler content, as shown in **Figure 5**a,b.

An important observation is that the values of s_0 in the non conductive samples (unfilled, 0.5CNT and 1CNT) cannot be obtained through the fitting procedure with Equation (3). Hence, the measured value of σ' at low frequency (i.e., 200 Hz) was taken as an approximate value for the samples containing a reinforcement concentration below the percolation threshold, i.e., when the σ_0 plateau cannot be appreciated in the experimental data. Obviously, the measured values overestimate the real σ_0 of the nonconductive samples, but they just serve to give an idea of the transition in the conductive behavior experienced by the samples. On the other hand, we also note that the values of electrical conductivity obtained for the samples above the percolation threshold are several orders of magnitude lower than those typically measured for individual carbon nanotubes (i.e., ≈105 S m^{-1},

see for example Kaneto et al.[44]). This is not unexpected, as the contact resistance among nanotubes and the presence of a non-conductive polymeric interphase should be also considered.[45,46]

Besides this, from Figure 5a, it is also interesting to note that the conductivity of the compounds with a CNT content above 4 phr is higher than that of the 40CB. Also, from this figure it could be estimated that ϕ_c has to be sought in the range of 1–3 phr of CNT. The trend exhibited by the critical exponent s also corroborates that range. Indeed, a value of $s \approx 1$ is characteristic of nonconductive materials exhibiting a typical capacitor behaviour, whereas $s < 1$ typically corresponds to conductive materials.[43] In particular, values of s in between 0.8 and 1 are characteristic of hopping in disordered materials.[47] Additional information about the AC conduction mechanism could be obtained by looking at the temperature dependence of the dielectric response, especially for what concerns the exponent s of Equation (3).[48]

The electrical percolation threshold was estimated using arguments based on percolation theory. The network of conductive particles is expected to exhibit a critical behavior at a CNT concentration j_c, above which s_0 as a function of ϕ can be represented by[49]

$$\sigma_0 = k(\phi - \phi_c)^t \qquad (4)$$

being k a scaling constant and t a parameter related to the electrical transport mechanism. The values of σ_0, obtained from Equation (3) and shown on Figure 5a, have been iteratively fitted above 2 phr of CNT, in the range of $1 > \phi_c > 3$ phr of CNT, incrementally varying the value of ϕ_c in 0.1 phr. The electrical percolation threshold has been identified as the value which returns the maximum regression coefficient. The final fitting is shown in **Figure 6** with the parameters obtained. The values of s_0 are aligned in a log–log plot, in agreement with Equation (4), and the electrical percolation threshold obtained is (1.6 ± 0.1) phr.

3.3. Dynamic Mechanical Analysis

Frequency dependence of the viscoelastic properties at different temperatures have been measured. First, the measurements made on the unfilled sample have analyzed and the data of the storage modulus and loss modulus (E' and E'', respectively) as a function of frequency at different temperatures are shown in **Figure 7**. As expected, the values increase as the temperature decreases due to slowing down of the thermal molecular motion, the effect being more pronounced for the loss modulus. Moreover, the T-dependence of both moduli is more evident above the glass transition temperature.[50]

For the unfilled compound, the E' curves measured at temperatures other than 0 °C have been shifted horizontally to superimpose them on the curve measured at 0 °C using the time–temperature superposition principle, resulting in the black square dots in **Figure 8**. From the values of the applied horizontal shifts, a_T (the subscript T indicates the dependence on the measurement temperature), as determined empirically, it is possible to obtain information on the elastomer structure through the values of parameters c^0_1 and c^0_2 defined from a best-fitting
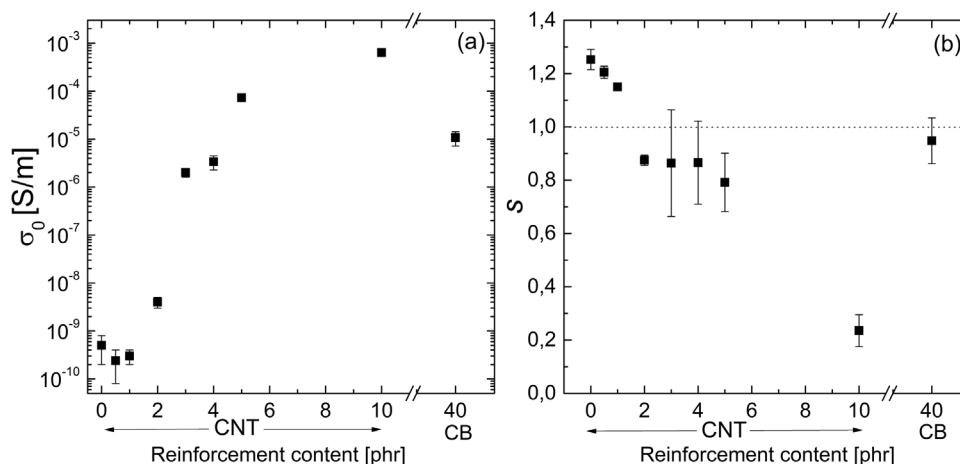
Figure 5. Estimated parameters obtained by fitting dielectric measurements represented on Figure 4 by Equation (3): a) extrapolated DC conductivity σ_0 and b) critical exponent s, both as function of the reinforcement content.
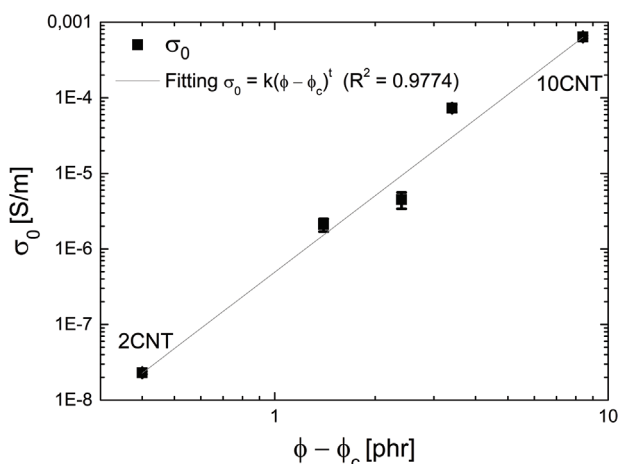
Figure 6. Extrapolated low-frequency real part of the complex conductivity as a function of the difference between the reinforcement content ϕ and the percolation threshold value ϕ_c (with $\phi > \phi_c$).

procedure of the shift factors using the well-known William–Landel–Ferry model (WLF model)[23]

$$\log a_T = -\frac{c_1^0 \left(T - T_0 \right)}{c_2^0 + T - T_0} \quad (5)$$

The horizontal shifts are represented in **Figure 9** as a function of the measurement temperature and it is evident that have been successfully fitted with Equation (5), obtaining $c_1^0 = 30.1$ and $c_2^0 = 202.7\,°C$ (the superscript indicates that these values are in correspondence to the value of the chosen reference temperature, $T_0 = 0\,°C$). To the best of our knowledge, no data are available in the literature about master curves on SBR at $T_0 = 0\,°C$. Klüppel analyzed SBR samples reinforced with CB and silica obtaining $c_1 = 7.7$ and $c_2 = 82.7\,°C$[51] for a master curve determined at 20 °C, a reference temperature different from the one used in this work.

It is possible to estimate the c parameters at a determined temperature using the following equations[52]

$$c_1^0 = \frac{c_1^1 c_2^1}{c_2^1 + T_0 - T_1} \quad (6.1)$$

$$c_2^0 = c_2^1 + T_0 - T_1 \quad (6.2)$$

where the superscript in the parameters c_1 and c_2 indicates the corresponding reference temperature. After applying those formulas to the values obtained by Klüppel ($T_1 = 20\,°C$, $c_1^1 = 7.7$ and $c_2^1 = 82.7\,°C$) to obtain the corresponding ones to $T_0 = 0\,°C$, the following values are obtained: $c_1^0 = 10.2$ and $c_2^0 = 62.7\,°C$. These values are lower than those obtained in the samples analyzed in this work. Nevertheless, the differences can be attributed to a different cure system, which gives a diverse network structure.

The constructed master curves for the unfilled sample are shown as black squares on E' and E'', in Figure 8a,b, respectively. The frequency range has been thus extended to 10^{-2}–10^4 Hz, a much wider range as compared to that of the original measurements that have been performed in the range 0.8–30 Hz (Figure 7).

By analyzing the T_g values obtained by DSC (Table 1), it can be seen that the transition from the glassy to the rubbery state occurs at similar temperature values for all the samples, independently of the filler content. This behavior is already reported by few works in the literature[10,51] and indicates that the relaxation spectrum during the glass transition is independent of reinforcement content and only depends on the rubber phase. This allows to use the values of the horizontal shift, a_T, already determined for the unfilled compound for the data of the reinforced samples in order to obtain the master curves for the filled samples. After this procedure, it has been observed that the curves do not overlap satisfactorily in the low frequency region, for both E' and E'', indicating that the time–temperature superposition principle is not fulfilled in reinforced samples in the region of low frequencies. In fact, in the case of reinforced rubber, at high frequencies (low temperature) the response is dominated by the polymer
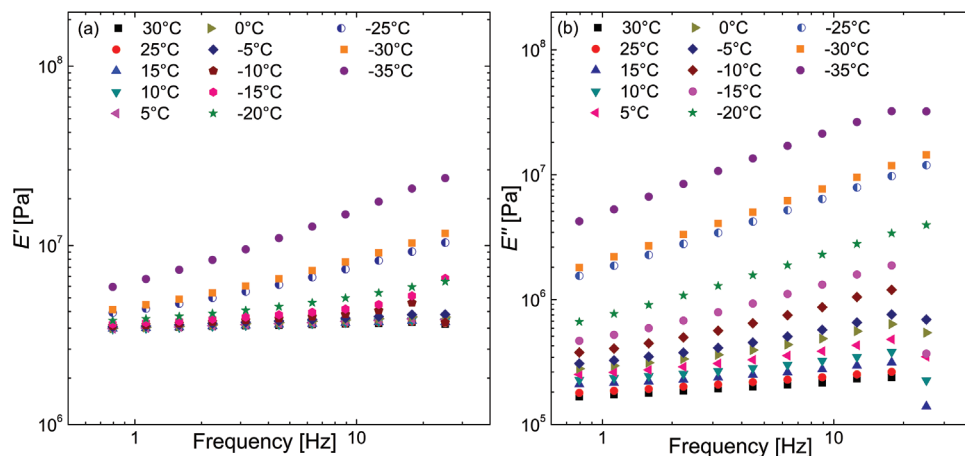
Figure 7. For the unfilled compound: frequency sweep of a) E' and b) E'' at different temperatures between −35 up to 30 °C.
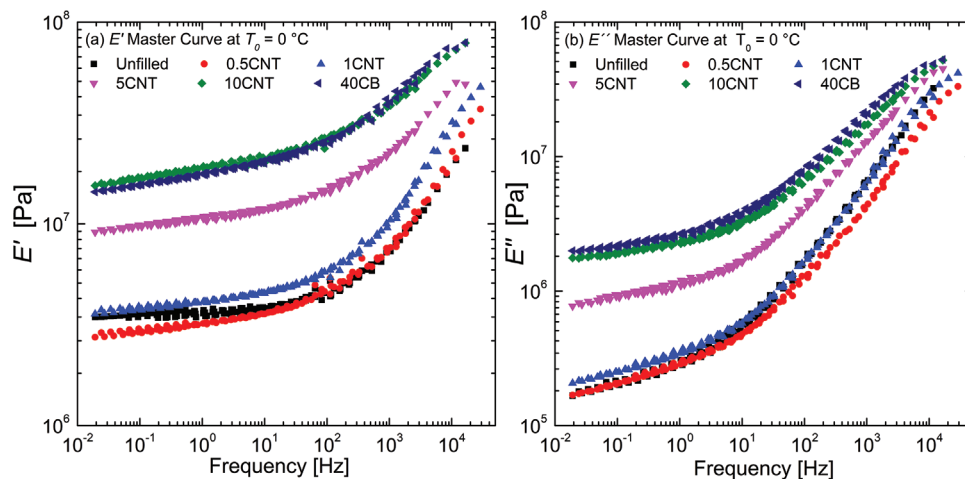
Figure 8. Master curves for the unfilled and all reinforced compounds performed at 0 °C as reference temperature: a) E' and b) E'' as function of frequency.
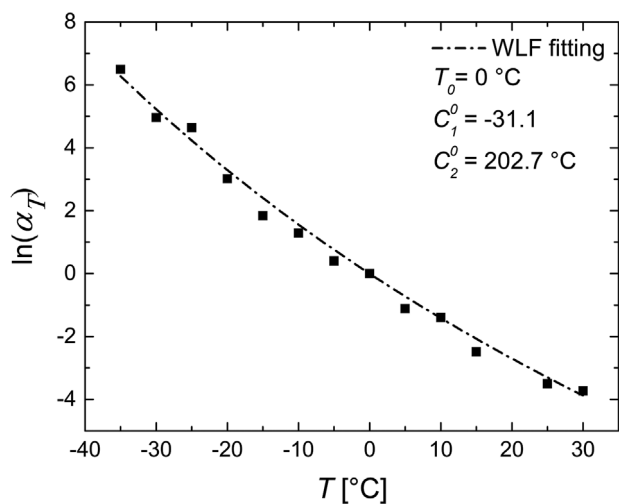
Figure 9. For the unfilled compound: Shift factor values applied on the E' at the corresponding temperatures T to perform the master curve at $T_0 = 0$ °C. The dashed line is the WLF fitting with Equation (5).

matrix. On the other hand, at low frequencies (high temperature) the matrix is softer than the filler network, and therefore the dynamic properties are dominated by the latter. It can be inferred that the dynamics of the microstructure is governed by a superposition of two relaxation processes, and one prevails over the other according to the external conditions (frequency or temperature).[34]

It is well known that in reinforced samples there are several possible interactions between the polymer chains and the reinforcement particles. In a previous work we analyzed these samples through rubber process analyzer (RPA) measurements and the Maier–Göritz model was applied to obtain information about the microstructure.[2,54] Using this method, it was possible to discriminate the response under a dynamic deformation among stable and unstable contributions to the reinforcement network and to the storage modulus. It was found that the unstable interactions are more relevant than the stable ones when the CNT content is higher than 5 phr. Among the stable bonds are the polymer chains connecting reinforcement particles, therefore those chains have a similar hardness and

**ADVANCED
SCIENCE NEWS**

www.advancedsciencenews.com

**[M] acro-
molecular
Materials and Engineering**

www.mame-journal.de

Table 2. E_{act} values associated with the bound rubber movement for E' and E' from dynamic-mechanical master curves and for E' under temperature sweeps.

Compound	E_{act} (v_T (E')) [kJ mol^{-1}]	E_{act} (v_T (E'')) [kJ mol^{-1}]	E_{act} ($T(E')$) [kJ mol^{-1}]
5CNT	1.5 ± 0.2	9.7 ± 0.5	3.19 ± 0.07
10CNT	1.0 ± 0.1	9.1 ± 0.6	5.64 ± 0.07
40CB	3.8 ± 0.3	10.8 ± 0.7	5.72 ± 0.05

constitutes glassy-like polymer bridges (filler–filler bonds). In the literature, a temperature dependence of those glassy-like polymer bridges was found, through a significant decrease of the storage modulus when the temperature increases.[10,51] This behavior is not connected to the matrix dynamics and it is the reason of the splitting observed at low frequencies of the master curve. Several authors proposed that a vertical shift factor (v_T) can be applied to obtain a master curve for each of the reinforced compound.[10,51,55] After applying that procedure, continuous and smooth master curves have been obtained for all the compounds in E' and E'' and are shown in Figure 8a,b, respectively. In both cases, the modulus increases with the incorporation of filler particles, being more significant the difference at low frequency when the filler network dominates the compound behavior.

As Fritzsche and Klüppel have shown for SBR reinforced with different types and concentration of CB, it is possible to assign an activation energy (E_{act}) associated to a thermal movement of the bound rubber that connects the reinforcement particles.[10] The authors suggest that those polymer chains are like in a "glassy state" because their mobility is highly hindered, and this phase is bigger in size and with a higher hardness at lower temperature. Since this dynamic process is thermally activated, it is possible to describe it by an Arrhenius plot, obtaining the activation energy.[10] In **Figure 10**a–e it has been estimated the E_{act} by an Arrhenius plot of the vertical shift factors applied to the master curves of E' and E'' of the reinforced compounds. It is worth noting that the data at low temperature are out of the linear regression, so that, they have been ignored in the fitting procedure (empty points). This phenomenon can be easily explained by the hardening of the polymer chains of the rubber matrix at low temperature which completely inhibit the movements of the bound rubber that connects the reinforcement particles. The obtained results are shown in columns 1 and 2 of **Table 2**, the values corresponding to the 0.5CNT and 1CNT samples have been excluded because, as it can be seen in Figure 10a,b, the E' linear regression gives a negative value of E_{act}, which does not make sense. Nevertheless, this result is not surprising due to the fact that those concentrations are under the estimated percolation threshold, therefore, glassy like polymer bridges were not formed. According to the microstructure of reinforced elastomers, the two E_{act} values associated to E' and E'' are related with the temperature dependence of two kinds of glassy-like polymer bridges (filler–filler bonds): the E_{act} associated with E' is related to the stiffness of filler–filler bonds in a virgin state, while E_{act} associated with E'' corresponds to the stiffness of softer filler–filler bonds in a damaged state, resulting from stress induced breakdown and reaggregation of filler–filler bonds during cyclic deformations.[51,56] This scenario is similar to that stated by the Maier–Göritz model that was applied in the already mentioned previous work.[2] This confirms that the viscoelastic response of glassy-like polymer bridges plays a significant role in understanding the structural dynamics of filler-reinforced elastomers. In Table 2 it can be seen that the $E_{act}(E')$ is lower than $E_{act}(E'')$ for all the compounds and the highest values correspond to the 40CB compound, indicating a stronger constraint in the polymer chains when interacting with CB than with CNT.

From the temperature dependence of the E' (**Figure 11**a), it can be seen that a thermal effect remains at high temperatures in the rubbery state, being more evident in samples with a high reinforcement amount. Therefore, it is possible to perform an Arrhenius plot (logarithmic E' vs T^{-1}) by a linear fitting in the rubbery state to estimate the apparent thermal E_{act} from the slope (Figure 11b). The obtained values of E_{act} are on Table 2, third column, indicating an increase with the CNT content. Also, similar values of E_{act} were estimated for the 10CNT and 40CB compounds, even with the different morphology of the particles and amount of them. The fact that the E_{act} values are similar in the 10CNT and 40CB samples could indicate that the surface available to interact with the rubber chains is overall comparable.

The decrease of the E' with increasing temperature can be explained by the viscoelastic response of the polymer chains located between adjacent reinforcement particles, being the former immobilized at the beginning. As was previously mentioned, the filler particles are not directly in contact, but are connected by glassy-like polymer bridges.[2,10] Consequently, the properties of that phase composed of glassy-like polymer bridges are temperature dependent and it becomes softer when the temperature increases. This phenomenon also occurs on the polymer chains attached to the filler surface, which present a gradient of mobility, having a higher stiffness when closer to the particle surface. According to the investigations that Fritzsche and Klüppel made on SBR compounds reinforced with different types of CB, they found that with decreasing temperature the layer around the filler aggregates increases in thickness and the cross section of the glassy-like polymer bridges becomes larger. Therefore, both effects implicate an increasing stiffness and stability of the connecting glassy-like polymer bridges.[10] Moreover, it is expected that a higher value of E_{act} implies a smaller gap distance (between the reinforcement particles) and that the polymer there located is more hindered in its mobility. This is also related with the fact that above the T_g the compound stiffness is governed by the filler network. Comparing the results presented in Table 2, the E_{act} estimated from the vertical shifting factors in E' are smaller than that obtained from the temperature-dependent measurements of E'.

4. Conclusions

SBR compounds with different amounts of carbon nanotubes were thermally and dynamically analyzed. The samples were compounded in a two-roll mill and vulcanized at 160 °C. Also, for comparison purposes, an unfilled sample and one with 40 phr of CB were made.
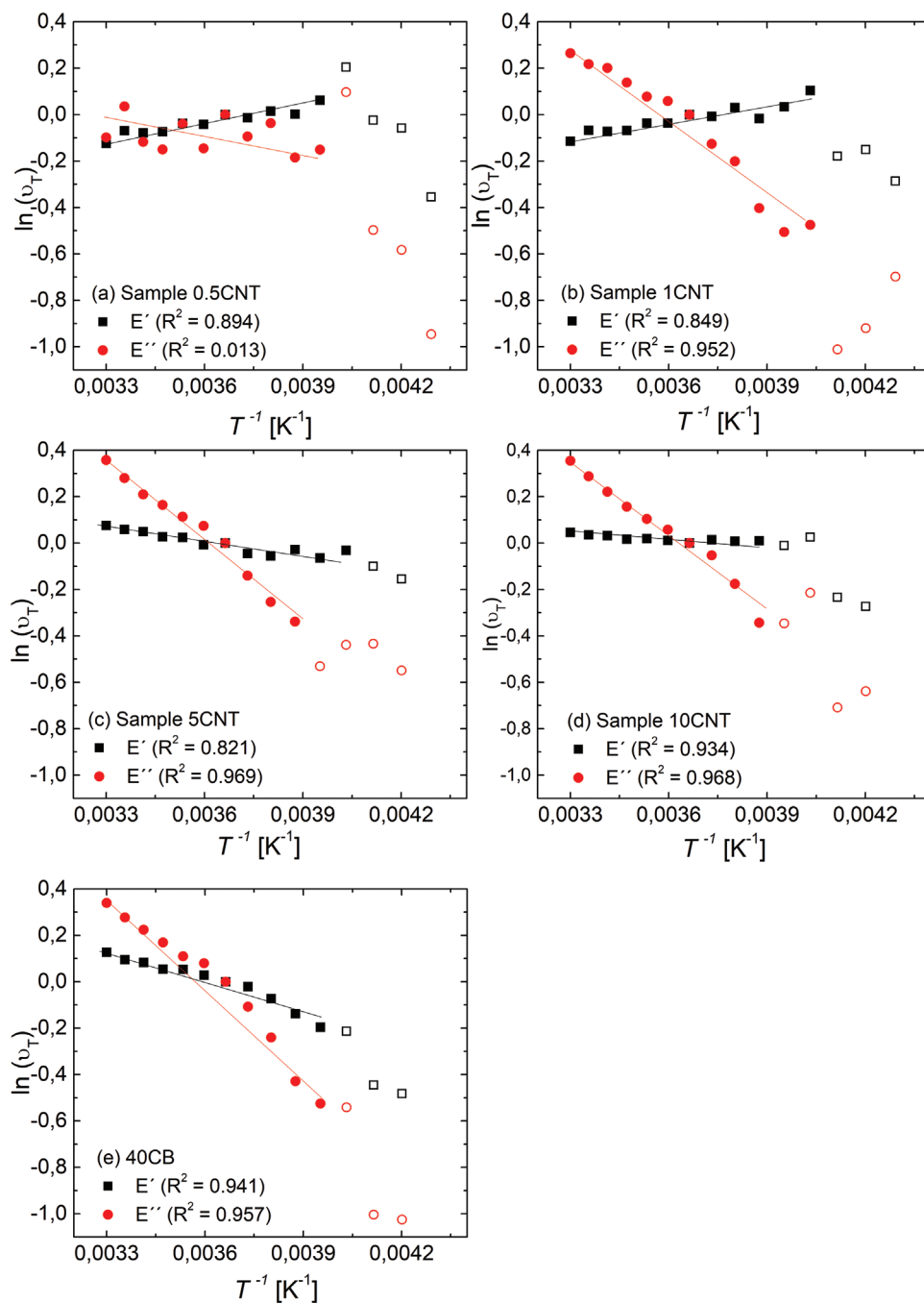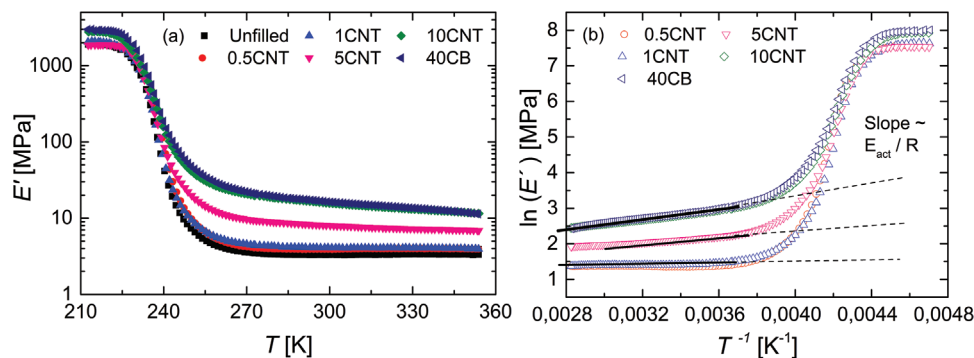
Figure 10. Vertical shift factors applied to get a continuous master curve of E' and E'' plotted as a function of the corresponding temperature of the measurement. The black line corresponds to an Arrhenius plot. a) 0.5CNT, b) 1CNT, c) 5CNT, d) 10CNT, and e) 40CB.

The DSC results indicated that the glass transition is dominated principally by the matrix due to the negligible differences observed in the values of the glass transition temperature for different CNT amount in the compound. Through the analysis of dielectric measurements, a (1.6 ± 0.1) phr concentration of CNT was estimated as the percolation threshold in the compounds.

From the dynamic measurements, the master curve of each compound was performed with 0 °C as reference temperature and the WLF equation was successfully applied on the horizon-

tal shifts. On the reinforced samples vertical shifting factors were necessary to obtain a continuous and smooth master curve. In particular, when the CNT concentration was above the percolation threshold, it was found a dependence of the vertical shifts with the temperature, which was associated with the thermal motion of the rubber chains between the reinforcement particles. Those polymer chains are like in a "glassy state" because their mobility is highly impeded, and this phase becomes bigger in size and acquires a higher hardness at lower temperature. Therefore,

**ADVANCED
SCIENCE NEWS**

www.advancedsciencenews.com

**Macro-
molecular
Materials and Engineering**

www.mame-journal.de

Figure 11. a) Temperature-dependence of E' measured by DMA, b) $\ln(E')$ as function of $T-1$ to perform an Arrhenius plot (dashed line) in the rubbery region for the compounds with a concentration over the percolation threshold: 5CNT, 10 CNT, and 40CB.

through an Arrhenius plot it was possible to estimate an activation energy associated with the thermal motion of those "glassy-like chains". According to the microstructure of a reinforced rubber, two types of E_{act} can be determined from the curves of E' and E'', which reflect the presence of two thermal mechanism on the glassy-like polymer bridges (filler–filler bonds): the E_{act} associated with E' is related to the stiffness of filler–filler bonds in a virgin state, while E_{act} associated with E'' corresponds to the stiffness of softer filler–filler bonds in a damaged state, resulting from stress induced breakdown and reaggregation of filler–filler bonds during cyclic deformations. The highest values were found on the compound with 40 phr of CB, which indicates a stronger interaction of the rubber chains with CB than with CNT.

Acknowledgements

Conflict of Interest

The authors declare no conflict of interest.

Data Availability Statement

The data that support the findings of this study are available from the corresponding author upon reasonable request.

Keywords

[1] D. García, M. Mansilla, M. Crisnejo, H. Farabollini, M. Escobar, *Polym. Eng. Sci.* **2019**, *59*, E327.
[2] D. B. Garcia, M. A. Mansilla, L. N. Monsalve, E. Bilbao, A. L. Rodríguez Garraza, M. M. Escobar, *J. Appl. Polym. Sci.* **2021**, *138*, 51362.
[3] S. Salaeh, A. Thitithammawong, A. Salae, *Polym. Test.* **2020**, *85*, 106417.
[4] S. K. Parameswaran, S. Bhattacharya, R. Mukhopadhyay, K. Naskar, A. K. Bhowmick, *J. Appl. Polym. Sci.* **2020**, *138*, 49682.
[5] A. Raju, B. Dash, P. Dey, S. Nair, K. Naskar, *Polym. Adv. Technol.* **2020**, *31*, 2390.
[6] J. A. Therattil, A. Kumar S, L. A. Pothan, H. J. Maria, N. Kalarikal, S. Thomas, *Macromol. Symp.* **2021**, *398*, 2000222.
[7] A. A. Mohammed, K. A. Sukkar, Z. Y. Shnain, *Chem. Pap.* **2021**, *75*, 3265.
[8] P. Bernal-Ortega, M. M. Bernal, A. González-Jiménez, P. Posadas, R. Navarro, J. L. Valentín, *Polymer* **2020**, *201*, 122604.
[9] J. B. Donnet, E. Custodero, in *Science and Technology of Rubber* (Eds: J. E. Mark, B. Erman, F. R. Eirich), Academic Press, CA, USA **2005**, Ch. 8.
[10] J. Fritzsche, M. Klüppel, *J. Phys.: Condens. Matter* **2011**, *23*, 035104.
[11] L. C. E. Struik, *Polymer* **1987**, *28*, 1521.
[12] G. Tsagaropoulos, A. Eisenburg, *Macromolecules* **1995**, *28*, 396.
[13] C. J. T. Landry, B. K. Coltrain, M. R. Landry, J. J. Fitzgerald, V. K. Long, *Macromolecules* **1993**, *26*, 3702.
[14] S. H. Anastasiadis, K. Karatasos, G. Vlachos, E. Manias, E. P. Giannelis, *Phys. Rev. Lett.* **2000**, *84*, 915.
[15] W. Tao, S. Zeng, Y. Xu, W. Nie, Y. Zhou, P. Qin, S. Wu, P. Chen, *Composites, Part A* **2021**, *143*, 106293.
[16] M. Marin-Genescá, J. García-Amorós, R. Mujal-Rosas, L. Massagués Vidal, X. C. Fajula, *Polymers* **2020**, *12*, 2675.
[17] A. Ahmadi, M. Asgari, *Int. J. Nonlinear Mech.* **2020**, *119*, 103364.
[18] J. Liu, B. Li, Y. Jiang, X. Zhang, G. Yu, C. Sun, S. Zhao, *Polym. Bull. (Heidelberg, Ger.)* **2022**, *79*, 87.
[19] H. Sun, X. Liu, B. Yu, Z. Feng, N. Ning, G. - H. Hu, M. Tian, L. Zhang, *Polym. Chem.* **2019**, *10*, 633.
[20] J. Liu, S. Wu, Z. Tang, T. Lin, B. Guo, G. Huang, *Soft Matter* **2015**, *11*, 2290.
[21] S. Wu, Z. Tang, B. Guo, L. Zhang, D. Jia, *RCS Adv.* **2013**, *3*, 14549.
[22] K. Subramaniam, A. Das, D. Steinhauser, M. Klüppel, G. Heinrich, *Eur. Polym. J.* **2011**, *47*, 2234.
[23] M. Rubinstein, R. Colby, *Polymer Physics*, Oxford University Press, Oxford, UK **2003**.
[24] K. Xiang, S. Wu, G. Huang, J. Zheng, J. Huang, G. Li, *Macromol. Res.* **2014**, *22*, 820.
[25] B. Shee, J. Chanda, M. Dasgupta, A. K. Sen, S. K. Bhattacharyya, S. Das Gupta, R. Mukhopadhyay, *J. Appl. Polym. Sci.* **2022**, *139*, 51950.

[26] L. H. Esposito, A. J. Marzocca, *J. Elastomers Plast.* **2022**, *54*, 169.

[27] J. Jung, H. A. Sodano, *J. Appl. Polym. Sci.* **2022**, *139*, 51856.

[28] S. K. Peddini, C. P. Bosnyak, N. M. Henderson, C. J. Ellison, D. R. Paul, *Polymer* **2014**, *55*, 258.

[29] G. Heideman, R. N. Datta, J. W. M. Noordermeer, B. Van Baarle, *Rubber Chem. Technol.* **2004**, *77*, 512.

[30] J. Wu, W. Xing, G. Huang, H. Li, M. Tang, S. Wu, Y. Liu, *Polymer* **2013**, *54*, 3314.

[31] E. Jafarpour, A. Shojaei, F. Ahmadijokani, *Polymer* **2020**, *196*, 122470.

[32] Z. Qian, J. Song, Z. Liu, Z. Peng, *Macromol. Res.* **2019**, *27*, 1136.

[33] P. A. Klonos, S. N. Tegopoulos, C. S. Koutsiara, E. Kontou, P. Pissis, A. Kyritsis, *Soft Matter* **2019**, *15*, 1813.

[34] C. Li, J. Wu, J. Zhao, D. Zhao, Q. Fan, *Eur. Polym. J.* **2004**, *40*, 1807.

[35] S. M. Hosseini, M. Razzaghi-Kashani, *Polymer* **2014**, *55*, 6426.

[36] X. Zhou, Y. Zhu, Q. Gong, J.i Liang, *Mater. Lett.* **2006**, *60*, 3769.

[37] L. Bokobza, *Polymer* **2007**, *48*, 4907.

[38] D. De Carvalho, D. Becker, C. Dalmolin, *J. Appl. Polym. Sci.* **2022**, *139*, e52656.

[39] N. Sermsook, N. Thummarungsan, K. Rotjanasuworapong, W. Lerdwijitjarud, A. Sirivat, *Sens. Actuators, A* **2022**, *344*, 113762.

[40] Z. - X. Huang, M. - L. Zhao, G. - Z. Zhang, J. Song, J. - P. Qu, *Compos. Sci. Technol.* **2021**, *212*, 108874.

[41] A. Bharati, M. Wübbenhorst, P. Moldenaers, R. Cardinaels, *Macromolecules* **2017**, *50*, 3855.

[42] A. Ameli, M. Nofar, C. B. Park, P. Pötschke, G. Rizvi, *Carbon* **2014**, *71*, 206.

[43] Y. C. Li, S. C. Tjong, R. K. Y. Li, *Synth. Met.* **2010**, *160*, 1912.

[44] K. Kaneto, M. Tsuruta, G. Sakai, W. Y. Cho, Y. Ando, *Synth. Met.* **1999**, *103*, 2543.

[45] W. S. Bao, S. A. Meguid, Z. H. Zhu, G. J. Weng, *J. Appl. Phys.* **2012**, *111*, 093726.

[46] Y. Zare, K. Yop Rhee, S. - J. Park, *Results Phys.* **2019**, *15*, 102562.

[47] J. C. Dyre, *J. Appl. Phys.* **1988**, *64*, 2456.

[48] F. Yakuphanoglu, I. S. Yahia, G. Barim, B. Filiz Senkal, *Synth. Met.* **2010**, *160*, 1718.

[49] D. Stauffer, A. Aharony, *Introduction to Percolation Theory*, Taylor & Francis, London, UK **2003**.

[50] H. G. H. Van Melick, L. E. Govaert, H. E. H. Meijer, *Polymer* **2003**, *44*, 2493.

[51] M. Klüppel, *J. Phys.: Condens. Matter* **2009**, *21*, 035104.

[52] J. D. Ferry, *Viscoelastic Properties of Polymers*, Wiley, Hoboken, NJ **1980**.

[53] A. Le Gal, X. Yang, M. Klüppel, *J. Chem. Phys.* **2005**, *123*, 014704.

[54] D. Göritz, H. Raab, J. Fröhlich, P. G. Maier, *Rubber Chem. Technol.* **1999**, *72*, 929.

[55] N. Chandran, C. Sarathchandran, S. Thomas, in *Rheology of Polymer Blends and Nanocomposites* (Eds: N. Chandran, C. Sarathchandran, S. Thomas), Elsevier, Amsterdam, Netherlands **2020**, Ch. 6.

[56] H. Lorenz, J. Fritzsche, A. Das, K. W. Stöckelhuber, R. Jurk, G. Heinrich, M. Klüppel, *Compos. Sci. Technol.* **2009**, *69*, 2135.